

**REPORT DOCUMENTATION PAGE***Form Approved*  
*OMB No. 0704-0188*

Public reporting burden for this collection of information is estimated to average 1 hour per response, including the time for reviewing instructions, searching existing data sources, gathering and maintaining the data needed, and completing and reviewing this collection of information. Send comments regarding this burden estimate or any other aspect of this collection of information, including suggestions for reducing this burden to Department of Defense, Washington Headquarters Services, Directorate for Information Operations and Reports (0704-0188), 1215 Jefferson Davis Highway, Suite 1204, Arlington, VA 22202-4302. Respondents should be aware that notwithstanding any other provision of law, no person shall be subject to any penalty for failing to comply with a collection of information if it does not display a currently valid OMB control number. **PLEASE DO NOT RETURN YOUR FORM TO THE ABOVE ADDRESS.**

<b>1. REPORT DATE (DD-MM-YYYY)</b> 09/28/2012			<b>2. REPORT TYPE</b> Final Technical Report			<b>3. DATES COVERED (From - To)</b> 08/01/2009 – 06/30/2012		
<b>4. TITLE AND SUBTITLE</b> Super-Critical Fuel Measurements						<b>5a. CONTRACT NUMBER</b> FA9550-09-C-0193		
						<b>5b. GRANT NUMBER</b>		
						<b>5c. PROGRAM ELEMENT NUMBER</b>		
<b>6. AUTHOR(S)</b> Gregory W. Faris						<b>5d. PROJECT NUMBER</b>		
						<b>5e. TASK NUMBER</b>		
						<b>5f. WORK UNIT NUMBER</b>		
<b>7. PERFORMING ORGANIZATION NAME(S) AND ADDRESS(ES)</b>  SRI International 333 Ravenswood Avenue Menlo Park, CA 94025-3493						<b>8. PERFORMING ORGANIZATION REPORT NUMBER</b> MP 12-004		
<b>9. SPONSORING / MONITORING AGENCY NAME(S) AND ADDRESS(ES)</b> AFOSR/RSA 875 Randolph Street Suite 325, Room 3112 Arlington, VA 22203-1768						<b>10. SPONSOR/MONITOR'S ACRONYM(S)</b>		
						<b>11. SPONSOR/MONITOR'S REPORT NUMBER(S)</b> AFRL-OSR-VA-TR-2012-1181		
<b>12. DISTRIBUTION / AVAILABILITY STATEMENT</b>  Approved for public release; distribution is unlimited								
<b>13. SUPPLEMENTARY NOTES</b>								
<b>14. ABSTRACT</b>  Work was performed on stimulated scattering for fuel property measurements at high temperatures and high pressures. The performance of a two-stage double-pass amplifier was improved to achieve required pulse energies and pulse lengths. Frequency modulation methods were developed to achieve rapid and sensitive stimulated scattering measurements. Frequency domain methods were developed to measure the refractive index to support conversion of spectroscopic parameters to physical parameters. System modifications were performed to convert the static measurement cell to a flowing cell. Stimulated Rayleigh scattering measurements were performed in JP-8 jet fuel. Analysis of high-temperature / high-pressure data in hexane provides evidence of the presence of an instability zone in the supercritical regime. Single-shot stimulated scattering measurements were performed with the stimulated Rayleigh scattering technique.								
<b>15. SUBJECT TERMS</b> Fuels, supercritical fluids, stimulated scattering, Brillouin scattering, Rayleigh scattering, elastic properties, thermal properties								
<b>16. SECURITY CLASSIFICATION OF:</b>				<b>17. LIMITATION OF ABSTRACT</b>  UL	<b>18. NUMBER OF PAGES</b>  20	<b>19a. NAME OF RESPONSIBLE PERSON</b> Dr. Chiping Li		
<b>a. REPORT</b> Unclassified	<b>b. ABSTRACT</b> Unclassified	<b>c. THIS PAGE</b> Unclassified	<b>19b. TELEPHONE NUMBER (include area code)</b> (703) 696-8574					

## Supercritical Fuel Measurements

Prepared by:

Gregory W. Faris  
Molecular Physics Laboratory

SRI Project P19112  
Contract Number FA9550-09-C-0193  
MP 12-004

Prepared for:

Air Force Office of Scientific Research

AFOSR/RSA  
875 Randolph Street  
Suite 325, Room 3112  
Arlington, VA 22203-1768

Attn: Dr. Chiping Li



**TABLE OF CONTENTS**

Objectives ..... 1

Status of Effort..... 1

Rationale ..... 1

Technical Discussion ..... 2

    Brillouin and Rayleigh Scattering ..... 3

    Stimulated Rayleigh-Brillouin Scattering ..... 3

    Stimulated Scattering - Experiment..... 6

    System Requirements ..... 6

    Laser System Modifications ..... 7

    Frequency Domain Measurement for Refractive Index Measurement ..... 8

    FM Stimulated Scattering Spectroscopy ..... 9

    Single Shot Measurements ..... 10

    Supercritical Cell and Fluid Handling ..... 11

    Supercritical Data ..... 12

Conclusions ..... 14

Personnel ..... 14

Publications ..... 14

Inventions/Discoveries ..... 14

References ..... 15

## **OBJECTIVES**

The long-term objectives of this project are to develop methods for measurements of fuel properties at high temperatures and high pressures and to apply these methods to jet fuel property measurements. The methods used for this work are stimulated Rayleigh and stimulated Brillouin scattering spectroscopy and a flowing high-pressure / high-temperature cell. Specific advances that enable these measurements include the use of a pulse-amplified laser system and frequency-modulation-stimulated scattering to provide sufficient spectral resolution for the measurements in the high-temperature and high-pressure regime.

## **STATUS OF EFFORT**

Work was performed on stimulated scattering for fuel property measurements at high temperatures and high pressures. The performance of a two-stage double-pass amplifier was improved to achieve required pulse energies and pulse lengths. Frequency modulation methods were developed to achieve rapid and sensitive stimulated scattering measurements. Frequency domain methods were developed to measure the refractive index to support conversion of spectroscopic parameters to physical parameters. System modifications were performed to convert the static measurement cell to a flowing cell. Stimulated Rayleigh scattering measurements were performed in JP-8 jet fuel. Analysis of high-temperature / high-pressure data in hexane provides evidence of the presence of an instability zone in the supercritical regime. Single-shot stimulated scattering measurements were performed with the stimulated Rayleigh scattering technique.

## **RATIONALE**

Better understanding of the behavior of supercritical fuels is important for advanced air-breathing propulsion systems and launch boosters. The unusual nature of these fuels requires detailed investigation of fuel behavior under anticipated conditions to ensure reliable vehicle performance. We are applying stimulated scattering to the measurement of the properties of supercritical fuels. The results of these studies will fill gaps in the understanding of fuel properties at supercritical conditions.

Fuel property measurements at high temperatures and pressures are performed using stimulated scattering methods,<sup>1-3</sup> which can be applied to any transparent material state. For example, we have applied stimulated scattering measurements to solids,<sup>3,6</sup> liquids,<sup>3,7,8</sup> gases,<sup>3</sup> and supercritical fluids.<sup>9</sup> Stimulated scattering methods have several advantages over other potential measurement methods. First, many properties can be measured with a single apparatus, including

density (from refractive index and absorption measurements), adiabatic compressibility (from speed of sound), viscosity (from acoustic damping rate), and thermal diffusivity (from thermal wave damping rate). Second, when coking occurs due to pyrolysis, optical (stimulated scattering) methods continue to work well, in contrast to conventional methods based on physical probes. For example, deposits onto torsion bars or hot wires affect the ability to perform viscosity or thermal conductivity measurements, respectively. Furthermore, perturbation of fluid properties by probes is avoided. Finally, the optical methods are able to perform measurements of fuel conditions and properties with high temporal and spatial resolution. The spatial resolution is  $\sim 100 \mu\text{m}$  transverse to the laser beam; this is the radial dimension for flow in a tube, which is the direction of the most rapid variation. The longitudinal dimension depends on the laser and flow cell geometry and is on the order of several mm to 1 cm. This is the direction of the flow, so slower variation is expected. With our latest innovation based on electronic tuning of the pump probe frequency shift and frequency modulation detection for stimulated scattering, the temporal resolution is  $\sim 1 \mu\text{s}$ , which is fast enough to freeze motion in supercritical fluids. Thus, the method can perform diagnostics on the heat transfer of high-temperature and high-pressure fuels, measuring the equation of state and the fuel properties in a manner not possible with other methods.

Stimulated scattering can be performed at any wavelength for which the material under study is transparent. For measurements on supercritical fuels, we perform stimulated scattering at a wavelength of  $1 \mu\text{m}$ . This wavelength is selected because spectral absorbance measurements performed on thermally stressed jet fuel show that although the fuel becomes quite dark in the visible region, it is still transparent in the near infrared (Figure 1).

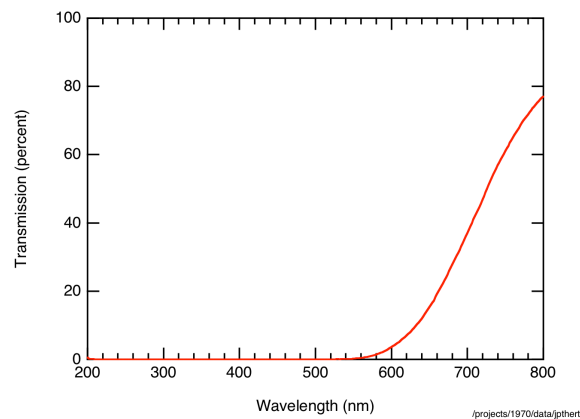


Figure 1. Transmission through 1 cm of JP-7 fuel, thermally stressed to  $1200^\circ\text{F}$ .

## TECHNICAL DISCUSSION

## BRILLOUIN AND RAYLEIGH SCATTERING

The elastic and inelastic scattering of light, including Rayleigh, Brillouin, and Raman scattering, arise from the natural oscillation modes of materials and can be used to determine the physical or chemical parameters responsible for those oscillations. These processes differ in energy lost in the scattering process as shown in Figure 2. A similar apparatus can measure these quite varied processes provided they cover the appropriate spectral range.

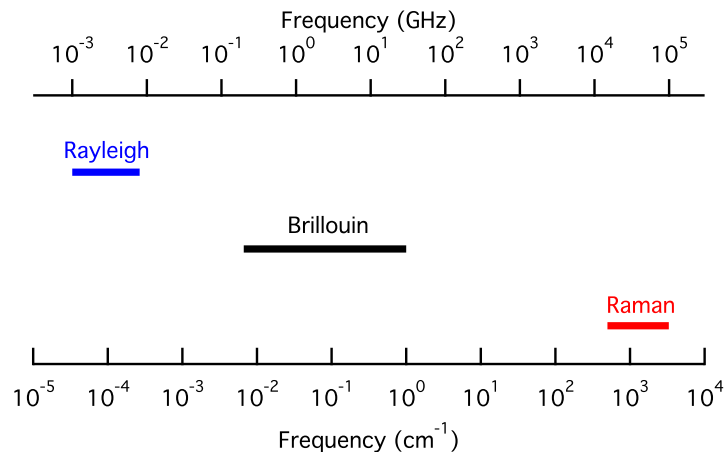


Figure 2. Frequency offset for different stimulated scattering processes.

We focus on Rayleigh and Brillouin scattering, which provide information on material physical properties. Rayleigh scattering results from refractive index variations due to thermal waves or diffusive density fluctuations and compositional fluctuations. Brillouin scattering results from refractive index variations due to sound waves or traveling density or pressure fluctuations. The Rayleigh-Brillouin scattering spectrum consists of three peaks. The form of the spontaneous Rayleigh-Brillouin spectrum is shown in Figure 3. The spectrum comprises a Rayleigh peak centered at the frequency of the incident laser beam and two Brillouin peaks shifted above and below the incident laser frequency by an amount proportional to the speed of sound.

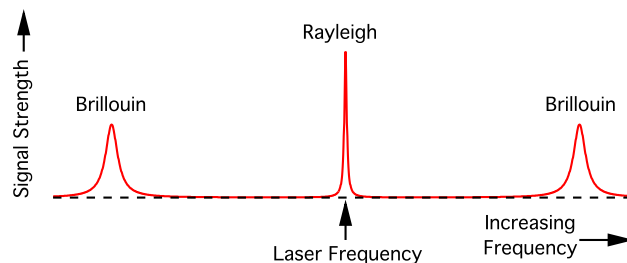


Figure 3. Diagram of spontaneous Rayleigh-Brillouin spectrum.

## STIMULATED RAYLEIGH-BRILLOUIN SCATTERING

When these collective modes are excited with a powerful laser, the mode oscillations can be driven so hard that they grow exponentially. This phenomenon is called stimulated scattering. We are applying stimulated Rayleigh and stimulated Brillouin scattering to measure thermal and elastic properties of fuels at high pressure and high temperature.

The dominant advantage of stimulated scattering is that the scattered signal can be made arbitrarily large; otherwise, the spontaneous forms of the scattering processes produce extremely weak signals. Thus, stimulated scattering measurements can provide very good signal-to-noise ratios. When using a probe beam to measure the induced amplification, we can obtain excellent quantitative results. This technique is distinct from the stimulated scattering that builds up from noise, in which case quantification is very difficult.

When using spontaneous scattering, discriminating between the Rayleigh or Brillouin scattered signals and the background excitation light can be quite difficult, even under ideal detection conditions. Discrimination is not a problem, however, for the stimulated scattering processes. Even though our measurements are performed within a few megahertz (a fraction of  $1 \text{ cm}^{-1}$ ) of the wavelength of the pulsed excitation laser, there is no contribution of scattered background light to the measurement.

Other advantages of stimulated scattering over spontaneous scattering include exceptional temporal resolution (with our new results, around  $1 \mu\text{s}$ ), much improved spectral resolution (limited by the laser linewidths rather than a spectrometer or interferometer), and very high signal-to-noise ratios. Furthermore, the use of two laser beams allows spatial registration and point measurement of local conditions.

The oscillatory mode forms in the region of overlap of the pump and probe laser beams as shown in Figure 4. The interference of the two laser beams produces density fluctuations in the form of a grating. This grating in turn scatters energy from one beam to the other when the appropriate detuning between the two laser beams meets a resonant condition. Other methods for measuring thermal and elastic properties exist, such as transient grating or forced scattering techniques.<sup>10-15</sup> Our method uses only two laser beams, so it is easier to align than these other methods, which require overlap of three lasers. Furthermore, phase matching is automatic once the two beams are overlapped, and only a single laser is required.

Two mechanisms can couple energy from light to matter for stimulated scattering: dipole forces (stimulated electrostrictive scattering) or light absorption (stimulated thermal scattering).<sup>7</sup> For electrostriction, the force of the electric field on induced dipoles in the material produces density variations. For absorption or thermal coupling, local heating due to absorbed light energy produces density variations. At our operational wavelength of 1064 nm, optical absorption can occur due to OH and CH overtone or combination bands.

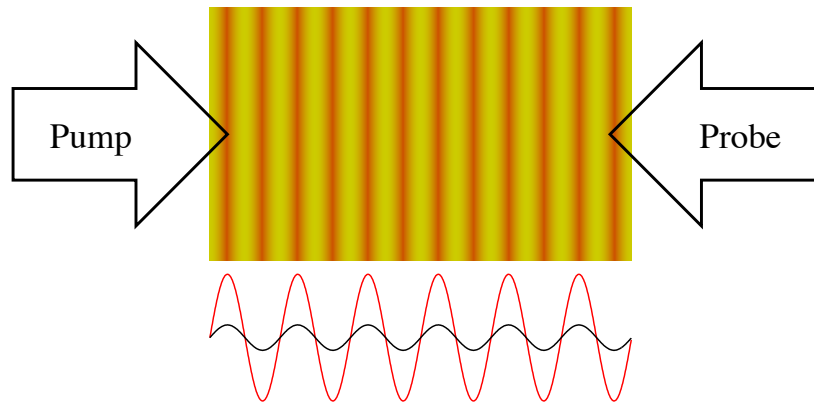


Figure 4. Beam interactions for stimulated scattering measurements.

Rayleigh/Brillouin spectroscopy provides information on a number of thermal and elastic physical properties through the dependence of the resonance positions, linewidths, and line strengths. The relationship between the dominant spectroscopic features and physical parameters are summarized in Table 1 and Figure 5. Not included are other features that may also appear in sensitive spectroscopic measurements near the laser frequency such as an additional oscillatory mode<sup>16,17</sup> that provides information about the exchange of energy between the internal vibrational modes and translational modes, and information on mixing or concentration gradients.<sup>18</sup>

Table 1. Physical parameters measured with Rayleigh/Brillouin spectroscopy

<b>Spectral Parameter</b>	<b>Physical Parameter</b>
Rayleigh width	Thermal diffusivity
Rayleigh height	Density / absorption <sup>a</sup>
Brillouin shift	Speed of sound / compressibility
Brillouin width	Acoustic damping rate / viscosity
Brillouin height	Density / absorption <sup>a</sup>

<sup>a</sup>For stimulated thermal scattering

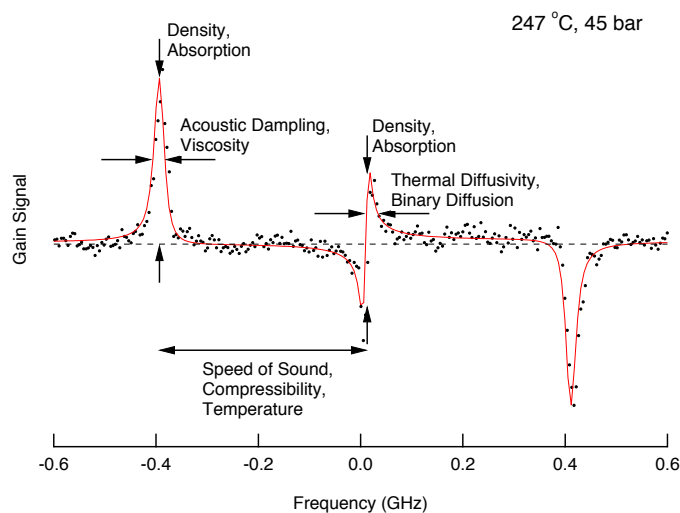


Figure 5. Spectrum of stimulated scattering showing relationship of spectroscopic properties and physical properties.

### STIMULATED SCATTERING - EXPERIMENT

The stimulated scattering measurements are performed in counter-propagating pump-probe geometry as shown in Figure 6. The measurement volume is defined by the intersection of the stronger pump laser with a weaker probe laser. Either laser may be tuned to obtain the Rayleigh/Brillouin spectrum. A 1064-nm pump laser sets up an electric polarization oscillating at the characteristic frequency of a scattering mode of the material.<sup>3</sup> For a strong input laser pulse, this polarization acts as a driving force, leading to amplification of both the material oscillation and a scattered optical wave. The optical amplification is detected as a gain or loss on the probe beam, which is provided by a continuous-wave (CW) laser.

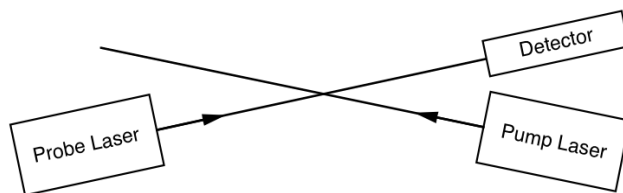


Figure 6. Schematic of pump-probe geometry for stimulated scattering measurements.

### SYSTEM REQUIREMENTS

We have applied stimulated scattering measurements to supercritical fluids.<sup>9</sup> In this work, we found four primary experimental improvements were necessary to perform accurate fuel property elements in the supercritical regime. First, knowledge of the refractive index is necessary to calculate accurate values of physical properties from spectroscopic properties. To meet this need, we have developed a frequency domain infrared radiofrequency (RF) interferometer (frequency domain instrument) similar to previous instruments we developed at

other wavelengths for other applications.<sup>19-21</sup> Second, in the supercritical regime, the stimulated Rayleigh line is too narrow to resolve with our existing apparatus because of the Fourier transform limit for the pulsed laser we were using. We have alleviated this concern by constructing a two-stage double-pass optical amplifier to pulse-amplify a narrowband fiber laser source. This new laser system is more than adequate to fully resolve the Rayleigh line in the supercritical regime.<sup>22</sup> Third, in certain portions of the supercritical regime, fluctuations lead to amplitude instabilities that can distort measured line shapes. We have overcome this limitation by developing a rapid scanning system that can acquire an entire stimulated scattering spectrum and 1  $\mu$ s or less, essentially freezing out the impact of any fluctuations on the measured line shapes.<sup>22</sup> Finally, our previous studies were performed in a static cell, which can create problems with coking from fuel pyrolysis during extended measurements. We have reconstructed our system to use a flow cell to alleviate this problem.

## LASER SYSTEM MODIFICATIONS

The experimental system has undergone significant changes since our initial studies.<sup>8,23</sup> The initial system used separate pump and probe lasers, with an external cavity diode laser as the probe laser and an injection-seeded Q-switched Nd:YAG laser as the pump laser. This was found to be inadequate for high-pressure / high-temperature studies because the Rayleigh linewidth is so narrow, on the order of a MHz<sup>9</sup>—a value that is small compared with both the drift between the frequencies of the pump and probe lasers and the Fourier-transform-limited linewidth of the Q-switched pump laser. The new system uses a single master oscillator for both pump and probe beams (Figure 7). The tuning between the pump and probe lasers is produced using frequency-offset generation. This essentially eliminates errors due to drift between the pump and probe lasers. A portion of the master oscillator beam is pulse-amplified in a two-stage double-pass Nd:YAG amplifier to produce the pump beam with a pulse length limited only by the flashlamp duration, or  $\sim 170$  microseconds. Use of a pulse-amplified laser instead of a Q-switched laser is possible because the peak power requirement for stimulated Rayleigh and stimulated Brillouin scattering is relatively low (about 1 kW).

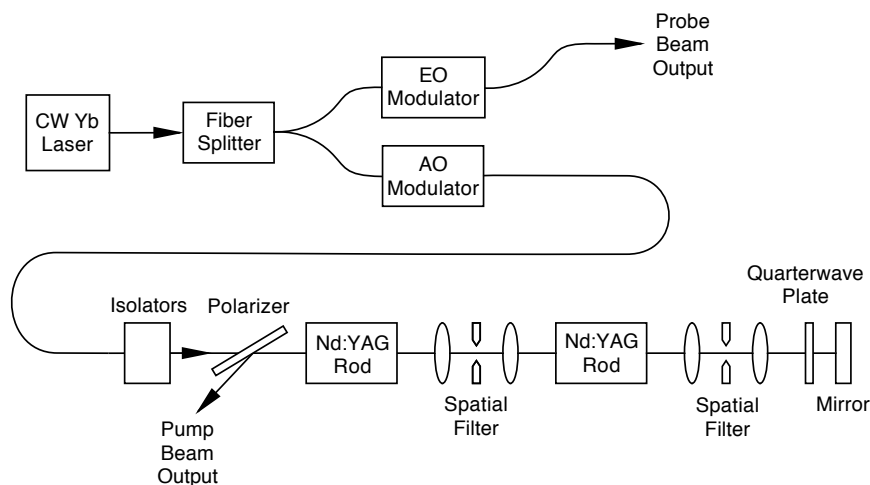


Figure 7. Schematic of current laser system for stimulated scattering.

We have had problems with self lasing in the four-stage Nd:YAG amplifier. This led to burning of components, including mirrors and fiber optics in the CW beam path. These were corrected by swapping metal mirrors for high-power dielectric mirrors and repolishing the fiber tips. However, to minimize system downtime and avoid possible damage to the fiber laser, we have added two additional optical isolators between the CW source and the pulsed Nd:YAG rods.

At various times, we have had hotspots in the output beam that were only present during pulsed operation and not when initial alignment was performed using the CW beam. Characterization of the hot spots using a camera-based laser beam profiler led us to believe that the hotspots are due to thermal lensing in the Nd:YAG rods during pulsed operation, causing slight misalignment through the spatial filters and producing fringing on the pinhole edges. The hotspots were eliminated by realignment of the laser rods with the CW beam only followed by careful realignment with the pulsed amplifiers on.

When testing for stimulated scattering using the long pulse operation ( $\sim 170$  microseconds), we found a thermal lensing signal in the sample that can confound the stimulated scattering signal. This lensing signal had not been a problem with earlier measurements at the shorter pulses. To overcome this effect, we have used the same acoustooptic modulator used to produce frequency shifts to select a short pulse from the CW beam, on the order of 1 to 30  $\mu\text{s}$  instead of the full pulselength governed by the flashlamp pumping. The shorter pulselength is sufficiently long to avoid spectral resolution limitations from the Fourier transform relation, since it is still roughly a factor of 100 times longer than our prior measurements. This pulse-slicing method is functioning well and is also advantageous because we can operate the laser at lower gains since the pulse-amplifier gain increases during the time that the CW lasers are switched off.

## **FREQUENCY DOMAIN MEASUREMENT FOR REFRACTIVE INDEX MEASUREMENT**

To use the Rayleigh and Brillouin shift information to calculate some thermal and elastic properties (i.e., convert from spectroscopic parameters to physical parameters), it is necessary to know the refractive index. We are applying a frequency domain system<sup>24-26</sup> at the same wavelength as the simulated scattering (1064 nm) to measure the refractive index. For the frequency domain method, light is RF amplitude modulated and the phase shift in the detected light is used to determine time delays for the light wave (Figure 8). In this case, we use the phase shifts of an amplitude modulated laser to determine refractive index. We have assembled an amplitude-modulated fiber-pigtail diode laser operating at 1064 nm as the basis of this method. This laser has been integrated with current and temperature control and has been tested for modulation up to 500 MHz. Operation beyond this point appears to be limited by either the bias tee on the laser mount or the laser itself. A 500-MHz modulation frequency provides ample sensitivity for our measurements. The overall system configuration is shown in Figure 9.

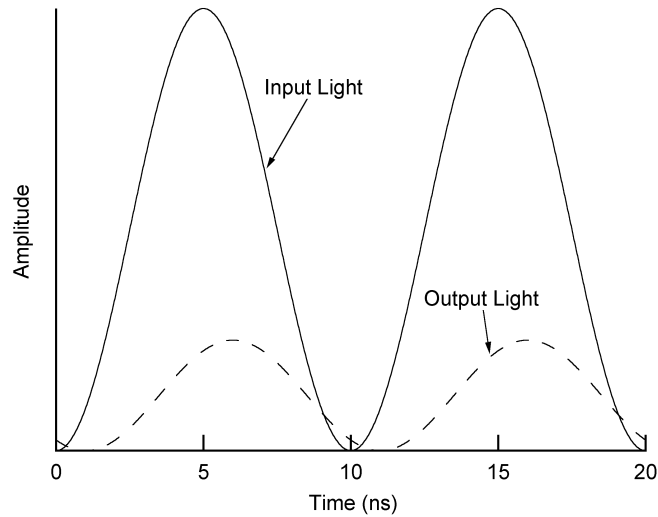


Figure 8. Schematic of frequency domain measurement of optical delay.

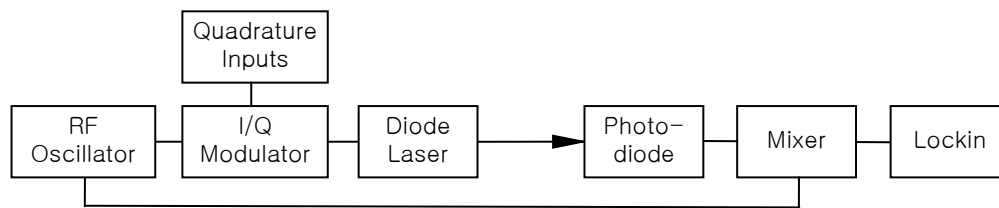


Figure 9. Instrumentation for frequency domain measurements.

## FM STIMULATED SCATTERING SPECTROSCOPY

Our measurements are based on the concept of FM spectroscopy.<sup>27-29</sup> Frequency modulation of a laser, for example using an electrooptic modulator, produces two sidebands, or additional frequencies offset from the central laser frequency ( $f_c$ ) by a fixed frequency above ( $f_c+f_m$ ) and below ( $f_c-f_m$ ) the central laser frequency. These two sidebands have opposite phases so that there is no net amplitude modulation. That is, when the FM beam is measured with a detector, the two sidebands cancel and there is no modulation on the measured signal. However, if an imbalance between the two sidebands is produced, then the two sidebands no longer cancel, and a net amplitude modulation is detected. In conventional FM spectroscopy, the imbalance between the two sidebands is produced by absorption. By varying the central frequency, a spectrum is obtained. Because of the cancellation effects of the two sidebands, the spectrum yields the first derivative of the actual spectrum.

FM spectroscopy can also be applied to stimulated Rayleigh/Brillouin scattering.<sup>30,31</sup> The cancellation of the two sidebands allows very sensitive measurements to be performed. We have performed the first application of FM stimulated scattering to Rayleigh scattering to our knowledge. An example for JP-8 jet fuel provided by Tim Edwards of Air Force Research Laboratory is shown in Figure 10. We measure two quadratures of the signal (I and Q, in top and

bottom of Figure 10), allowing determination of both amplitude and phase. Using a value for the refractive index  $n = 1.443$  for the JP-8 sample measured with an Abbe-3L refractometer (Bausch & Lomb), we calculate a value for the thermal diffusivity for JP-8 of  $7.3 \times 10^{-8} \text{ m}^2/\text{s}$ . This value agrees well with values expected from conventional measurements.<sup>32</sup> The sensitivity of the stimulated Rayleigh signals to the pump/probe phase is shown in Figure 11.

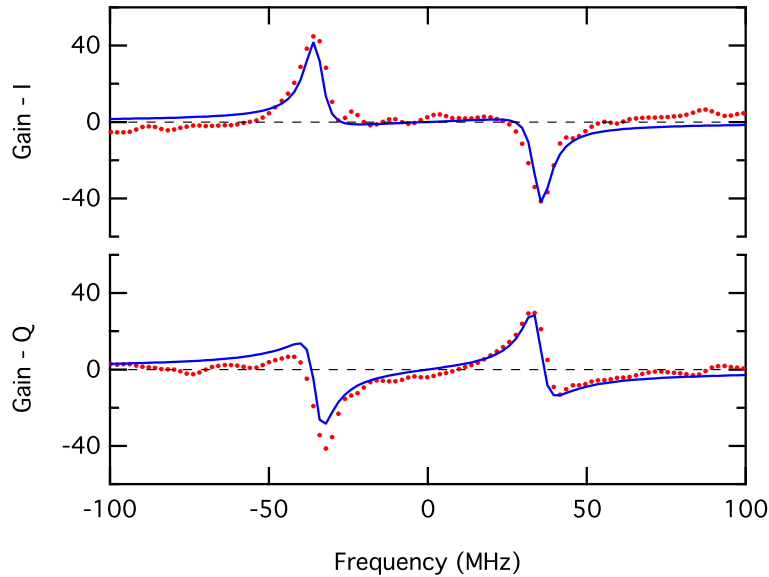


Figure 10. FM stimulated Rayleigh scan in JP-8 showing in-phase (I) and quadrature (Q) signals as a function of laser detuning. Data (red) and fit to theoretical model (blue) are shown.

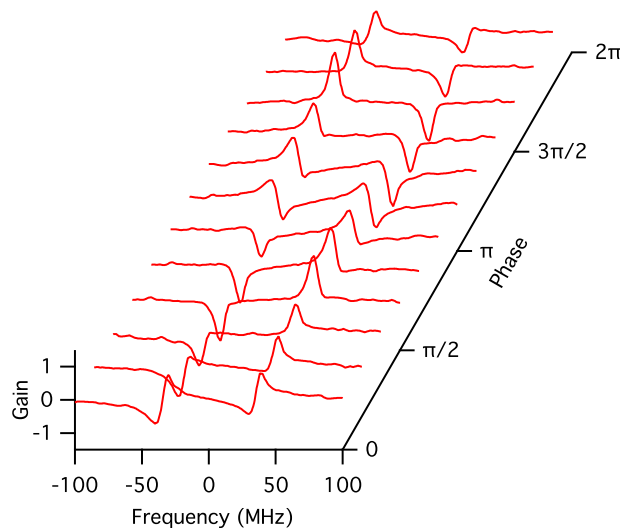


Figure 11. Variation of stimulated scattering signal with phase between pump and probe.

## SINGLE SHOT MEASUREMENTS

Since tuning between the pump and probe beam is performed electronically rather than by physically changing the laser cavities, the tuning can be performed very rapidly. We have recently demonstrated rapid tuning over an entire spectrum within a single laser pulse of 1 to 20  $\mu\text{s}$ .<sup>31</sup> We can tune the Rayleigh/Brillouin spectrum in a microsecond or less.

We have improved the signal-to-noise ratio for our current experimental apparatus through electronics improvements and control of stray light and have obtained what are to our knowledge the first single-shot stimulated scattering spectra. An example is shown in Figure 12(a). This pair of I/Q single-shot stimulated Rayleigh spectra was acquired in 20 microseconds with a peak power of 50 W (average power of 10 mW at 10 shots/s). For comparison, the average of 600 single-shot spectra (1 minute average) is shown in Figure 12(b).

Fit parameters for the single-shot data agree with the averaged data very well (see Table 2). The single-shot fitting results are much better than would be expected from the signal-to-noise ratio at a single point because the fit parameters are derived from all the points simultaneously.

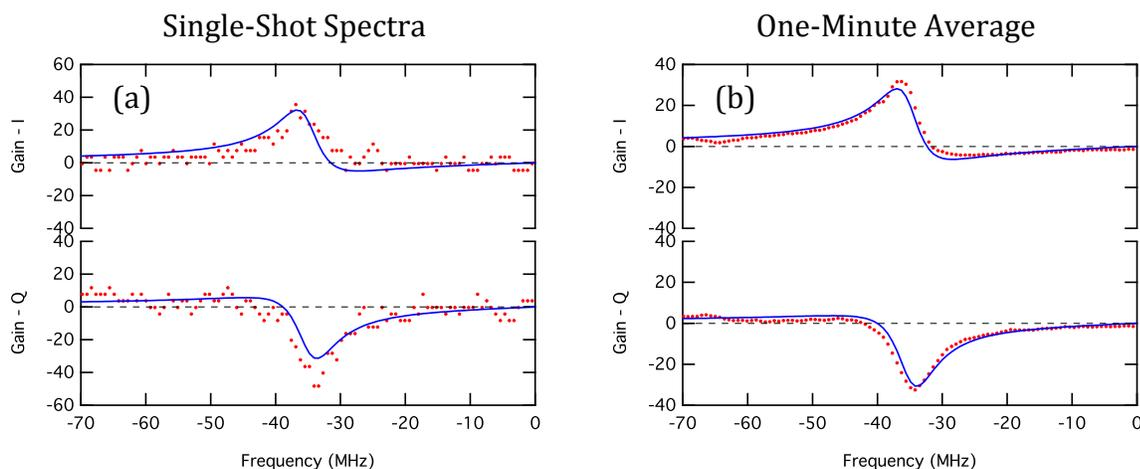


Figure 12. Single-shot (left) and one-minute averaged (right) spectra for hexane. Red points are data, blue lines are spectral fits.

Table 2. Comparison of Fit Parameters

	Width (MHz)	Shift (MHz)	Amplitude (mV)	Phase (rad)
Single Shot	7.28	-35.4	37.4	2.43
One Minute Average	7.24	-35.0	34.7	2.57
Deviation	0.5%	1.2%	7.7%	-0.14

## SUPERCritical CELL AND FLUID HANDLING

Previous supercritical measurements were performed in a static supercritical cell. Static systems are inadequate for supercritical fuel measurements because of degradation of the fuel for periods of longer than a few minutes.<sup>33,34</sup> Our new design uses a flow-through system. Our original static system was pressurized using a syringe pump and heated using a tube furnace. We

have replaced the syringe pump with a high-pressure liquid chromatography (HPLC) pump. The pump is operated at a constant flow, and the pressure controlled through a backpressure regulator at the system outlet. A cooling section following the cell prevents autoignition of the exiting fluid.

The optical cell has not been modified. Flow in the cell is currently directed across the windows and will keep fresh fluid flowing across the window surfaces when flow is applied. The cell windows are held in place with screws, allowing the windows to be easily removed for cleaning when necessary. Heating is performed using a tube furnace, as was done before. The current to the furnace is regulated by a temperature controller that monitors thermocouples in the optical cell inside the furnace. To adapt for a flowing system, preheating of the fuel is required before it enters the cell. This preheating of the fuel is performed using a coil of stainless steel tubing within the same furnace. The cell and spool for the preheat coil are shown in Figure 13. This figure shows the supercritical cell at the center with two aluminum spacers on either side. The spacer at the right has been cut down to allow wrapping 1/8 inch o.d. stainless steel tubing, which provides preheating the fuel to the same temperature as the cell.



Figure 13. Photograph of cell for supercritical studies.

## **SUPERCritical DATA**

High-temperature, high-pressure fluid measurements show a peak for stimulated Brillouin scattering along the extrapolation of the subcritical liquid/gas phase boundary. Calculations show this behavior appears due to inherent fluid properties rather than spectroscopic properties. These measurements can elucidate fluctuations along this extrapolated phase boundary and help identify potential zones of instability.

Measurements of the stimulated Brillouin peak height in n-hexane under supercritical conditions are shown at the top left of Figure 14 as a function of temperature and pressure. The location of the critical point for n-hexane is indicated by the red dot. The solid red line shows the

liquid-gas phase boundary below the critical point. Note that a peak in the Brillouin height is observed along the “Widom” line, or extension of the phase transition above the supercritical point (dashed red line). The nature of this structure in the high-pressure and high-temperature regime is not entirely understood. Similar plots of the Brillouin shift and Brillouin width over the same range of pressures and temperatures showed no similar structure (bottom left and bottom right of Figure 14). This is surprising since these are some of the key parameters involved in the Brillouin height. Beginning with the theoretical expression for the Brillouin gain<sup>3</sup> and making some simple scaling relationships, the Brillouin peak heights should scale approximately as the ratio of the Brillouin width to Brillouin shift times the electrostrictive coupling coefficient. If we make a plot of ratio of the Brillouin width to Brillouin shift (Figure 14 top right), we find a very similar pattern to that of the Brillouin heights. The fact that the agreement is not exact is not surprising given that this is only an approximate scaling relationship. Nevertheless, the nature of the agreement between the Brillouin peak heights and the Brillouin width to Brillouin shift ratio indicates that the local maxima in the Brillouin heights is likely due to physical properties rather than the electrostrictive coupling coefficient.

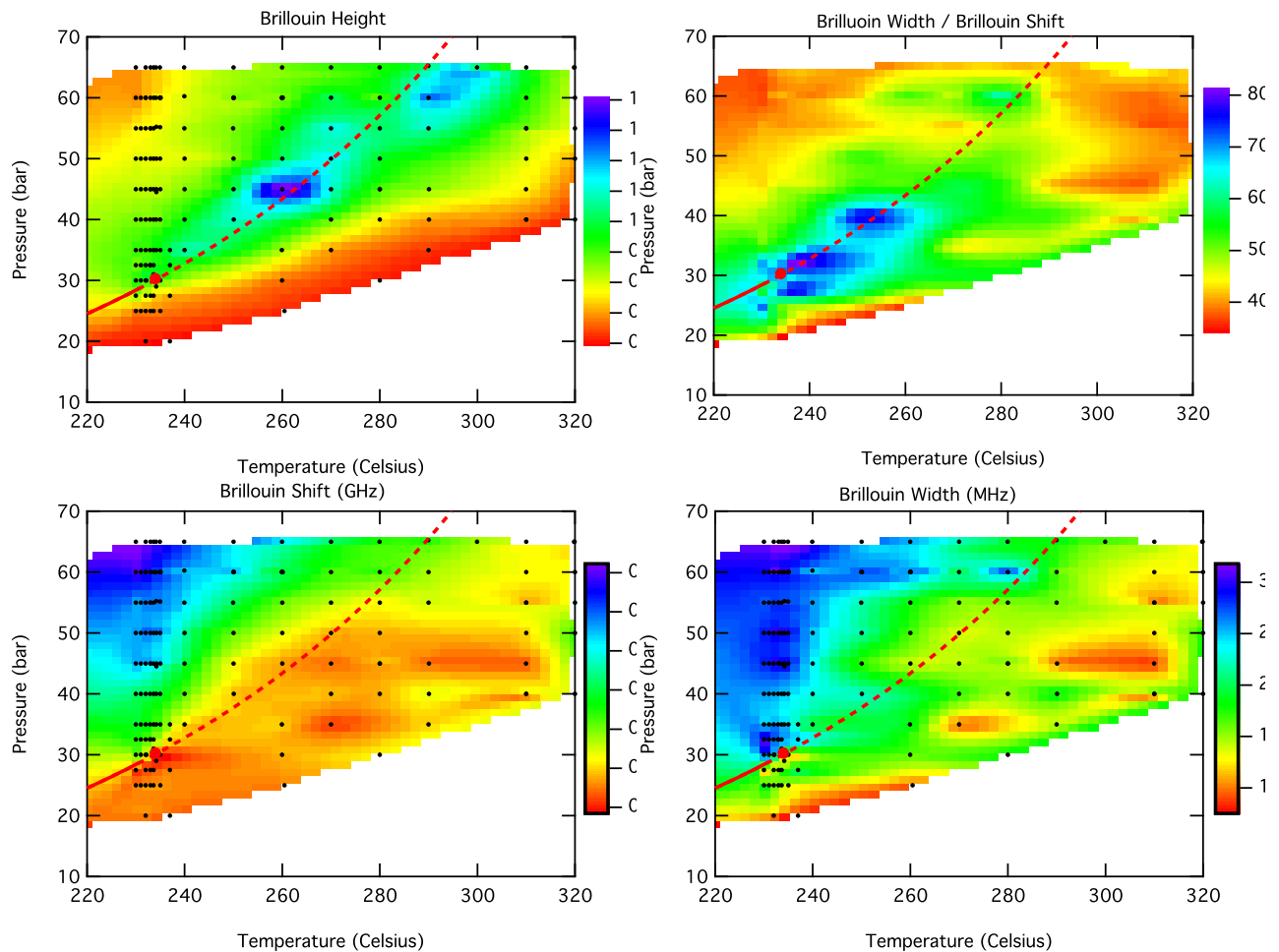


Figure 14. Plots of Brillouin height (top left, arbitrary units) and ratio of Brillouin width to Brillouin shift (top right, MHz/GHz), Brillouin shift (bottom left), and Brillouin width (bottom right).

## CONCLUSIONS

Stimulated scattering provides a good method for measurement of the physical properties of supercritical fuels. A range of properties can be measured with a single, relatively simple apparatus. High signal-to-noise ratios are achieved with modest laser powers (around 100 W peak power). Very rapid scans are possible using electronic laser tuning. We have made improvements to the method to obtain better measurements on supercritical fuels. These include high-spectral-resolution measurements based on a two-stage double-pass optical amplifier to fully resolve the stimulated Rayleigh peak in the supercritical regime, a frequency domain method for refractive index measurements to convert spectroscopic parameters to physical parameters, very rapid ( $\sim 1 \mu\text{s}$ ) scans to avoid measurement bias due to instabilities in the supercritical regime, and modification of the supercritical apparatus to support flow-through measurements to prevent buildup of pyrolyzed fuel on the optical windows. We have studied the line of instability in the supercritical regime. We have demonstrated single-shot measurement of stimulated Rayleigh scattering spectra.

## PERSONNEL

The following personnel contributed to the research on this project.

Gregory Faris, Program Manager, principal investigator and lead experimentalist

Ashot Markosyan, Experimental Physicist, consultant

Chia-Pin Pan, Postdoctoral Fellow, experimentalist

Steven Young, Mass Spectroscopy Specialist, electronics support, HPLC instrumentation

William Olson, Engineering Assistant Mechanical, mechanical support

Sage Doshay, Undergraduate Student, experimentalist

Christina L. Porter, Undergraduate Student, experimentalist

Jocienne Nelson, Undergraduate Student, experimentalist

## PUBLICATIONS

“Two-tone frequency modulation stimulated Rayleigh scattering,” manuscript in preparation.

## INVENTIONS/DISCOVERIES

Electronic offset stimulated scattering (in process).

## REFERENCES

1. W. Kaiser and M. Maier, "Stimulated Rayleigh, Brillouin, and Raman spectroscopy," in *Laser Handbook*, F. T. Arecchi and E. O. Schulz-Dubois, Eds. (North-Holland, Amsterdam, 1972), Vol. 2, pp. 1077-1150.
2. R. W. Boyd, "Stimulated Brillouin and Stimulated Rayleigh Scattering," in *Nonlinear Optics* (Academic Press / Elsevier, Burlington, MA, 2008), pp. 429-471.
3. G. W. Faris, L. E. Jusinski, and A. P. Hickman, "High-resolution stimulated Brillouin gain spectroscopy in glasses and crystals," *J. Opt. Soc. Am. B* **10**, 587-599 (1993).
4. G. W. Faris, "Brillouin gain spectroscopy in glasses and crystals," in *Applied Laser Spectroscopy*, W. Demtröder and M. Inguscio, Eds. (Plenum Press, New York, 1990), pp. 307-312.
5. G. W. Faris, L. E. Jusinski, M. J. Dyer, W. K. Bischel, and A. P. Hickman, "High-resolution Brillouin gain spectroscopy in fused silica," *Opt. Lett.* **15**, 703-705 (1990).
6. G. W. Faris, M. J. Dyer, and A. P. Hickman, "Transient effects on stimulated Brillouin scattering," *Opt. Lett.* **17**, 1049-1051 (1992).
7. G. W. Faris, M. Gerken, C. Jirauschek, D. Hogan, and Y. Chen, "High-spectral-resolution stimulated Rayleigh-Brillouin scattering at 1  $\mu\text{m}$ ," *Opt. Lett.* **26**, 1894-1896 (2001).
8. C. Jirauschek, E. M. Jeffrey, and G. W. Faris, "Electrostrictive and thermal stimulated Rayleigh spectroscopy in liquids," *Phys. Rev. Lett.* **87**, 233902 (2001).
9. K. S. Kalogerakis, B. H. Blehm, R. E. Forman, C. Jirauschek, and G. W. Faris, "Stimulated Rayleigh and Brillouin scattering in a supercritical fluid," *J. Opt. Soc. Am. B* **24**, 2040-2045 (2007).
10. H. Eichler, G. Enterlein, P. Glozbach, J. Munschau, and H. Stahl, "Power requirements and resolution of real-time holograms in saturable absorbers and absorbing liquids," *Appl. Opt.* **11**, 372-375 (1972).
11. H. Eichler, G. Salje, and H. Stahl, "Thermal diffusion measurements using spatially periodic temperature distributions induced by laser light," *J. Appl. Phys.* **44**, 5383-5388 (1973).
12. D. W. Pohl, S. E. Schwarz, and V. Irniger, "Forced Rayleigh scattering," *Phys. Rev. Lett.* **31**, 32-35 (1973).
13. D. E. Govoni, J. A. Booze, A. Sinha, and F. F. Crim, "The non-resonant signal in laser-induced grating spectroscopy of gases," *Chem. Phys. Lett.* **216**, 525-529 (1993).

14. S. Williams, L. A. Rahn, P. H. Paul, J. W. Forsman, and R. N. Zare, "Laser-induced thermal grating effects in flames," *Opt. Lett.* **19**, 1681-1683 (1994).
15. M. S. Brown, Y. Y. Li, W. L. Roberts, and J. R. Gord, "Analysis of transient-grating signals for reacting-flow applications," *Appl. Opt.* **42**, 566-578 (2003).
16. R. D. Mountain, "Spectral distribution of scattered light in a simple fluid," *Review of Modern Physics* **38**, 205-214 (1966).
17. W. S. Gornall, G. I. A. Stegeman, B. P. Stoicheff, R. H. Stolen, and V. Volterra, "Identification of a new spectral component in Brillouin scattering of liquids," *Phys. Rev. Lett.* **17**, 297-299 (1966).
18. R. P. C. Schram, G. H. Wegdam, and A. Bot, "Rayleigh-Brillouin light-scattering study of both fast and slow sound in binary gas mixtures," *Physical Review A: Atomic, Molecular, and Optical Physics* **44**, 8062-8071 (1991).
19. M. Gerken and G. W. Faris, "High-precision frequency-domain measurements of the optical properties of turbid media," *Opt. Lett.* **24**, 930-932 (1999).
20. M. Gerken and G. W. Faris, "Frequency-domain immersion technique for accurate optical property measurements of turbid media," *Opt. Lett.* **24**, 1726-1728 (1999).
21. M. Gerken, D. Godfrey, and G. W. Faris, "Frequency-domain technique for optical property measurements in moderately scattering media," *Opt. Lett.* **25**, 7-9 (2000).
22. G. W. Faris, A. Markosyan, and C. L. Porter, "Stimulated Rayleigh scattering using a single laser source," Manuscript in preparation (2012).
23. C. Jirauschek, E. M. Jeffrey, and G. W. Faris, "Electrostrictive and thermal stimulated Rayleigh spectroscopy in liquids," *Phys. Rev. Lett.* **87**, 233902 (2001).
24. B. Chance, M. Cope, E. Gratton, N. Ramanujam, and B. Tromberg, "Phase measurement of light absorption and scatter in human tissue," *Rev. Sci. Instrum.* **69**, 3457-3481 (1998).
25. S. Fantini and M. A. Franceschini, "Frequency-domain techniques for tissue spectroscopy and imaging," in *Handbook of Optical Biomedical Diagnostics*, V. V. Tuchin, Ed. (SPIE Press, Bellingham, WA, 2002), pp. 405-453.
26. A. E. Cerussi and B. J. Tromberg, "Photon migration spectroscopy frequency-domain techniques," in *Biomedical Photonics Handbook*, T. Vo-Dinh, Ed. (CRC Press, Boca Raton, 2003), pp. 22-21-22-17.
27. G. C. Bjorklund, "Frequency-modulation spectroscopy: a new method for measuring weak absorptions and dispersions," *Opt. Lett.* **5**, 15-17 (1980).

28. C. B. Carlisle, D. E. Cooper, and H. Preier, "Quantum noise-limited FM spectroscopy with a lead-salt diode laser," *Appl. Opt.* **28**, 2567-2576 (1989).
29. U. Gustafsson, G. Somesfalean, J. Alnis, and S. Svanberg, "Frequency-Modulation Spectroscopy with Blue Diode Lasers," *Appl. Opt.* **39**, 3774-3780 (2000).
30. T. Sonehara, Y. Konno, H. Kaminaga, S. Saikan, and S. Ohno, "Frequency-modulated stimulated Brillouin spectroscopy in crystals," *J. Opt. Soc. Am. B* **24**, 1193-1198 (2007).
31. G. W. Faris, A. Markosyan, and C. L. Porter, "Two-tone frequency modulation stimulated Rayleigh scattering," Manuscript in preparation (2012).
32. T. J. Bruno, M. L. Huber, A. R. Laesecke, E. W. Lemmon, M. O. McLinden, S. L. Outcalt, R. A. Perkins, B. L. Smith, and J. A. Widegren, Thermodynamic, Transport, and Chemical Properties of Reference JP-8, NIST Interagency/Internal Report (NISTIR) - 6659 (July 14, 2010).
33. T. Edwards, "personal communication," (2006).
34. T. Edwards, "Cracking and deposition behavior of supercritical hydrocarbon aviation fuels," *Combust. Sci. Technol.* **178**, 307-334 (2006).